

“Orphan” afterglows in the Universal Structured Jet Model for γ -ray bursts

Elena M. Rossi^{1,2}, Rosalba Perna^{1,3} & Frédéric Daigne^{4,5}

¹ *JILA, University of Colorado at Boulder, 440 UCB Boulder, CO 80309-0440*

² *Chandra Fellow*

³ *Department of Astrophysical and Planetary Sciences, University of Colorado*

⁴ *Institut d’Astrophysique de Paris, UMR 7095 CNRS – Université Pierre et Marie Curie-Paris VI, 98 bd Arago, 75014 Paris, France.*

⁵ *Institut Universitaire de France*

e-mail: emr@jilau1.colorado.edu (EMR), rosalba@jilau1.colorado.edu (RP) daigne@iap.fr (FD)

6 February 2020

ABSTRACT

The paucity of reliable achromatic breaks in Gamma-Ray Burst afterglow light curves motivates independent measurements of the jet aperture. Orphan afterglow (OA) searches, especially at radio wavelengths, have long been the classic alternative. These survey data have been interpreted assuming a uniformly emitting jet with sharp edges (“top-hat” jet), in which case the ratio of nearly isotropic afterglows to GRBs scales with the jet solid angle. Data could so far only loosely constrain the jet size. We consider, instead, an almost isotropic outflow with a luminosity that decreases across the emitting surface. The total GRB energy can be lower than for an isotropic top-hat jet, and the current lack of positive detections can be more easily explained. In particular, we adopt the universal structured jet (USJ) model, that reproduces the observed afterglow phenomenology to the same extent as the top-hat jet. However, the interpretation of the OA data is very different if GRBs are described by the USJ rather than the top-hat model. We compute, within the framework of the USJ, the number and rate of orphan afterglows expected in all-sky snapshot observations as a function of the survey sensitivity. We find that the current (negative) results for OA searches are in agreement with our expectations. In radio and X-ray bands this was mainly due to the low sensitivity of the surveys, while in the optical band the sky-coverage was not sufficient. A comparison with the top-hat model is also performed. In general we find that X-ray surveys are poor tools for OA searches, if the jet is structured. On the other hand, the FIRST radio survey and future instruments like the Allen Telescope Array (in the radio band) and especially GAIA and Pan-Starrs (in the optical band) will have excellent chances, not only to detect OAs, but also to put strong constraints on the jet models.

1 INTRODUCTION

Surveys for transient sources may detect Gamma-Ray Burst (GRB) afterglows. In this paper, we call an “orphan” afterglow any afterglow associated with such serendipitous searches, as opposed to “triggered” GRB afterglows, localized through the preceding prompt γ -ray emission. Rhodes (1997) suggested that these surveys could be used to put constraints on the geometrical beaming angle of the GRB jets in the “top-hat” (thereafter TH) model. In this model, GRBs are assumed to be uniformly emitting within a cone of angle θ_{jet} with sharp edges, where the luminosity drops suddenly to an undetectable level.

The suggestion by Rhodes (1997) is based on the fact that the prompt γ -ray emission is relativistically beamed within an angle $\theta_{\text{jet}} + 1/\Gamma$, where $1/\Gamma \ll \theta_{\text{jet}}$. Thus, if the line of sight lies outside this angle, the GRB is not detected. However, as the outflow slows down in the afterglow phase,

the visible region increases to eventually encompass the observer’s line of sight. At late times, $\Gamma \sim 1$ and the emission is roughly isotropic. Therefore with ideal detectors, more long-wavelength transients than γ -ray ones should be expected. In the limit of infinitely sensitive instruments, the ratio of (nearly isotropic) OAs to triggered GRB afterglows (or prompt events) is given by the beaming factor $b \propto \theta_{\text{jet}}^{-2}$. A measure of this quantity would be of great importance as it would allow one to calibrate θ_{jet} and then estimate the true GRB rates ($\propto b$) and energetics ($\propto b^{-1}$).

Searches for OAs have been performed at various wavelengths, but none of them has yielded a firm detection. Several authors have used observations in the radio band to constrain the GRB rate and energetics (e.g. Perna & Loeb 1998; Woods & Loeb 1999; Paczyński 2001; Levinson 2002; Gal-Yam et al. 2006), since late time (i.e. nearly isotropic) afterglow emission peaks in this band. The simplest and most common assumption is that the predicted number of OAs in

a snapshot observation is *proportional* to the beaming factor. Perna & Loeb (1998) used the lack of detections to set an upper limit of $b \lesssim 10^3$. More recently, Levinson et al. (2002) and Gal-Yam et al. (2006) compared their data with a more detailed model for radio afterglows. They showed that the number of expected OAs in a flux limited survey is *inversely* proportional to b and they place a lower limit of $b \gtrsim 60$.

X-ray survey data have been used to search for OAs by Grindlay (1999) and by Greiner et al. (2000), while optical searches have been more numerous (Schaefer et al. 2002; Vanden Berk et al. 2002; Becker et al. 2004; Rykoff et al. 2005; Rau et al. 2006; Malacrino et al. 2007). Using shorter wavelengths than radio to constrain the beaming factor necessarily requires a careful comparison with theoretical predictions (e.g. Totani & Panaitescu 2002; Nakar, Piran & Granot 2002), since the emission is likely to be still relativistically beamed when OAs are detected in those bands. Malacrino et al. (2007, 2007b) put the tightest optical constraints so far (see their fig.3). Their non-detection resulted in an upper limit for the number of OAs on the sky that is marginally consistent with the predictions of Totani & Panaitescu (2002) and consistent with Nakar et al. (2002) and Zou et al. (2007).

The purpose of this paper is to show that the interpretation of the results of the searches for OAs is very different if GRB jets do not have a “top-hat structure”. Numerical simulations of collapsing massive stars (e.g. MacFadyen & Woosley 1999) show that the jet emerges from the star with an energy distribution $E(\theta)$ and Lorentz factor $\Gamma(\theta)$ that vary as a function of the angle θ from the jet axis. It has been shown (Rossi, Lazzati & Rees 2002; Zhang & Mészáros 2002) that, if $E(\theta) \propto \theta^{-2}$ the diversity of afterglow light curves can be ascribed to different viewing angles within the context of an universal structured jet (USJ). In the USJ model, the outflow is assumed to be geometrically isotropic and composed of a brighter uniform spine surrounded by wings that become dimmer and dimmer away from the jet axis. The isotropic feature is attractive since it may explain the lack of OA detections, while the non-uniform energy distribution allows one to avoid the huge energy requirement demanded by GRBs with an isotropic equivalent energy $\gtrsim 10^{54}$ ergs (e.g. GRB 990123). In this model $b = 1$.

In this paper, we use the USJ framework to compute the expected number of transients in an all-sky snapshot and their rate as a function of the survey sensitivity. The aim is pursued by means of Monte Carlo simulations of the afterglow properties, as observed by X-ray, optical and radio surveys. The procedure is described in § 2. We compare our results with the top-hat predictions (§ 3.1). Finally, we review prospects for OA detections with current and future surveys (§ 3.2). This allows us to identify the best survey characteristics to increase the chance of detection and single out the most promising future missions. We discuss and conclude our work in § 4.

2 SIMULATING THE POPULATION OF ORPHAN AFTERGLOWS

We use Monte Carlo methods to simulate the population of GRB orphan afterglows in the USJ. GRBs are randomly generated on the sky with a probability distribution in redshift

that traces the star formation rate (SFR) (§ 2.1). We use the external shock model to compute the afterglow luminosity curve (§ 2.2). The probability function for the viewing angle θ is given by the fraction of the solid angle associated with that angle, $P(\theta) \propto \sin(\theta)$. Our simulation yields for radio, optical and X-ray bands the distribution of afterglow fluxes and the total number of afterglows on the sky for a snapshot observation, together with the average time T_{th} that an afterglow remains detectable in the sky, as a function of the detection threshold. Finally, we compute the OA detection rate for any flux limited survey where the observation time is much greater than T_{th} .

2.1 Formation rate and γ -ray luminosity function

We assume that the GRB population in the universe is described by a redshift-independent luminosity function and a redshift distribution.

In the USJ, the isotropic equivalent kinetic energy in the afterglow phase has the angular dependence

$$E(\theta) = \frac{E_c}{1 + \left(\frac{\theta}{\theta_c}\right)^2}, \quad (1)$$

where the bright central spine with angular size θ_c has a maximum kinetic energy $E_c = E(0)$. The expected luminosity function follows from $P_{\text{GRB}}(L) = P(\theta) \frac{d\theta}{dL}$ (Rossi et al. 2002),

$$P_{\text{GRB}}(L) \propto \frac{\sin\left(\theta_c \sqrt{\frac{L_c}{L} - 1}\right)}{\sqrt{\frac{L_c}{L} - 1}} \left(\frac{L_c}{L}\right)^2, \quad (2)$$

where L [erg s⁻¹] is the isotropic equivalent bolometric peak luminosity and L_c is proportional to E_c (see eq. 3). In equation 2, we assume that the γ -ray emission efficiency and the ratio of mean luminosity to peak luminosity is independent of the angle.

The GRB comoving rate $R_{\text{GRB}}(z)$ [yr⁻¹ Mpc⁻³] is assumed to follow the comoving rate $R_{\text{SN}}(z)$ [yr⁻¹ Mpc⁻³] of Type II supernovae. We assume that these arise from stars with masses above $8 M_{\odot}$ and that the initial mass function has a Salpeter form (e.g. Porciani & Madau 2001). Daigne, Rossi & Mochkovitch (2006, thereafter DRM06) found that the above prescription is dubious for redshift greater than 2. However, most of the OAs that are detected in a survey are located at lower redshifts, where this assumption appears to hold. In our analysis, we find, in fact, that the mean OA redshift for any reasonable flux threshold is never greater than $z = 2$. The star formation rate we adopt to derive R_{SN} (dubbed SFR₂) and its comparison with data (Hopkins 2004) are shown in fig. 1 of DRM06. This SFR saturates beyond $z \sim 2$ at a level of $0.2 M_{\odot} \text{ yr}^{-1} \text{ Mpc}^{-3}$. Even though this behavior is consistent with data at the one sigma level, the flat extrapolation of our SFR after the peak remains questionable, since high- z data are plagued by uncertainty on the amount of dust extinction. However, we do not expect that uncertainties in the high- z behavior of $R_{\text{GRB}}(z)$ appreciably affects our results. The GRB redshift probability function is thus obtained as an integral over redshift of $R_{\text{GRB}}(z)$ times the comoving volume, taking into account time dilation.

The free parameters for the luminosity function and for

the redshift distribution are $k \equiv \frac{R_{\text{GRB}}}{R_{\text{SN}}}$, L_c and θ_c . We constrained them by fitting simultaneously: i) the $\log N - \log P$ distribution of GRBs (where P [ph cm $^{-2}$ s $^{-1}$] is the peak flux) detected by the Burst and Transient Source experiment (BATSE; Kommers et al. 2000; Stern et al. 2000, 2002); ii) the peak energy distribution of bright BATSE bursts (Preece et al. 2000); and iii) the HETE2 fraction of X-ray rich GRBs and X-ray flashes (Sakamoto et al. 2005). The parameter values are optimized by χ^2 minimization. This procedure was previously used by DRM06, where a detailed description of the code can be found. In particular, among their options, we choose to describe the γ -ray spectrum with a log-normal distribution for the peak energy (see their § 2.3). The results for the best fit are $\log(k) = -5.99 \pm 0.06$, $\log(L_c[\text{erg s}^{-1}]) = 53.7 \pm 0.6$ and $\theta_c = 9.2 \pm 5.2^\circ$. The reduced $\chi^2 = 1.53$ for 37 degrees of freedom. We note here that DRM06, assuming a power-law luminosity function, found ~ -1.6 as the best fit value for the slope when this is free to vary, as opposed to ~ -2 (eq. 2). However, an acceptable χ^2 is also obtained in our case.

2.2 Physical description of afterglow lightcurves

The afterglow emission is modeled as synchrotron radiation from a relativistic blast-wave propagating in a constant density external medium (e.g. Mészáros & Rees 1997). We ignore the contribution from the reverse shock, since although it dominates the afterglow emission in the first few tens of seconds after the GRB (Sari & Piran 1999), OA observations occur much later. For the same reason, our results are largely independent of the choice of the initial Lorentz factor (which we fix at $\Gamma_0 = 300$), since the deceleration time is unlikely to exceed 10^3 s (e.g. Panaitescu & Kumar 2000). Similar consideration of timing allow us to neglect the modelling of the early afterglow features (flares, plateau, etc., e.g. Nousek et al. 2006), that are not reproduced by the standard external shock model.

The code we use for the calculation is described in Rossi et al. (2004). For each lightcurve, L_a [erg s $^{-1}$ Hz $^{-1}$], the input parameters are: the angular distribution of kinetic energy, the viewing angle, the shock parameters, the external density and the rest-frame frequency.

The luminosity function parameters, L_c and θ_c , constrained by the prompt emission data (§ 2.1) allow us to determine the kinetic energy distribution within the jet (eq. 1), since

$$E_c \propto \left(\frac{1 - \eta_\gamma}{\eta_\gamma} \right) L_c. \quad (3)$$

Inspection of current data suggests that the proportionality constant is of the order of 1 second. The γ -ray efficiency η_γ that is inferred from modeling data in the standard external-internal shock scenario is rather high, between $\sim 50\%$ and $\sim 90\%$ (Panaitescu & Kumar 2002). This uncertainty together with the one σ range of L_c imply $10^{52} \lesssim E_c [\text{erg}] \lesssim 2 \times 10^{54}$. We adopt $E_c = 1.3 \times 10^{53}$ erg. Since the core angle is not strongly constrained by prompt emission data (see 2.1), we adopt a value at the low end of the one σ range, $\theta_c = 4^\circ$, to account for the observed breaks in the lightcurves on day timescales. The external shock and density parameters are chosen from the ranges of values inferred from afterglow modeling (e.g. Panaitescu & Kumar

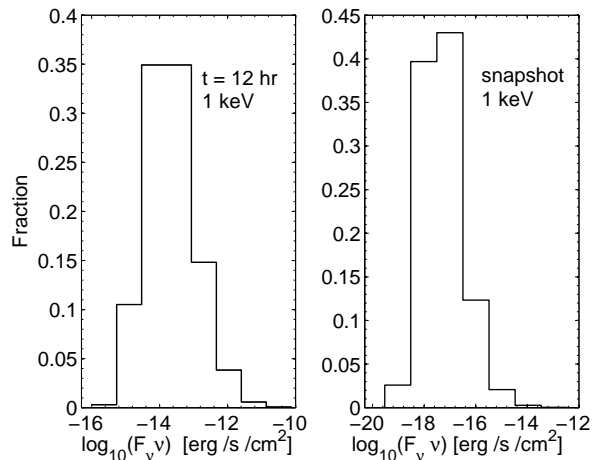


Figure 1. Flux distribution in the X-ray band at 1 keV energy; these distributions are intrinsic, i.e. no selection criteria have been applied. *Left panel:* the distribution of fluxes at 12 hours after the trigger. This may be compared with fig. 5 of Berger et al. (2005), taking into account that their observed distribution suffers from selection effects. *Right panel:* the flux distribution as it appears in a snapshot observation of the sky.

2001). The fraction of energy at the shock that goes into accelerated electrons and magnetic field is $\epsilon_e = 0.05$ and $\epsilon_B = 0.005$ respectively; the electrons are accelerated into a power-law with exponent $p = 2.2$. The external number density is taken to be $n = 1$ cm $^{-3}$. The whole set of parameters (E_c , θ_c , ϵ_e , ϵ_B , p and n) yield results consistent with the observed afterglow flux distributions (Berger et al. 2005). Our flux distributions are shown in Fig. 1 to Fig. 3. In the right panels, we plot the histogram of fluxes in a given band for all afterglows detected in a snapshot observation of the sky. In the left panels, we show the flux histogram of the same afterglows evaluated at a common observed time. These latter distributions compare favorably with fig. 4, fig. 5 and fig. 6 of Berger et al. (2005)¹.

We compute afterglow lightcurves $L_a(\nu \times (1+z), \theta, t')$ for three observed frequencies, $\nu = 2.42 \times 10^{17}$ Hz (1 keV), $\nu = 4 \times 10^{14}$ Hz (R band) and $\nu = 5 \times 10^9$ Hz; 6 redshifts, $0 \leq z \leq 20$; 10 viewing angles, $0^\circ \leq \theta \leq 90^\circ$ and 57 comoving times t' , spanning 10 years. We arrange those data in the form of a matrix that can be easily interpolated in order to assign a luminosity L_a to each simulated burst. The flux observed on Earth is calculated from L_a with $H_0 = 73$, $\Omega_\Lambda = 0.72$ and $\Omega_M = 0.24$ (Spergel et al 2006). Examples of lightcurves are shown in Fig. 4: in this example the GRB is situated at $z=1$ and viewed under different angles, in our three bands of observation.

2.3 Monte Carlo code for “Orphan” Afterglows

To model the OA population, GRBs are randomly generated with a flat distribution backward in time from the snapshot

¹ We do not attempt a formal quantitative comparison with data, since this would require us to take into account selection effects in different bands that are difficult to quantify.

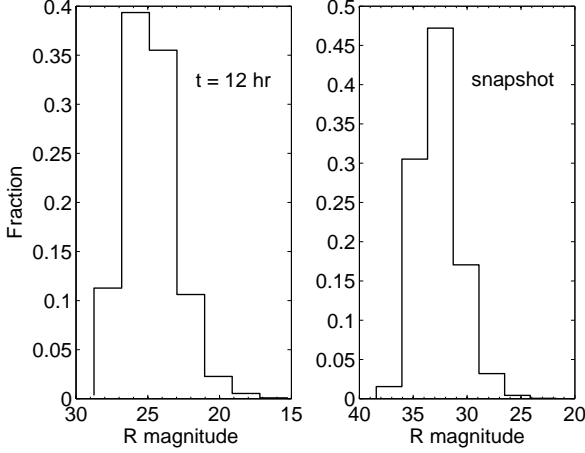


Figure 2. As Fig. 1 but for magnitude distributions in the R band. Our left panel may be compared with fig. 4 of Berger et al. (2005)

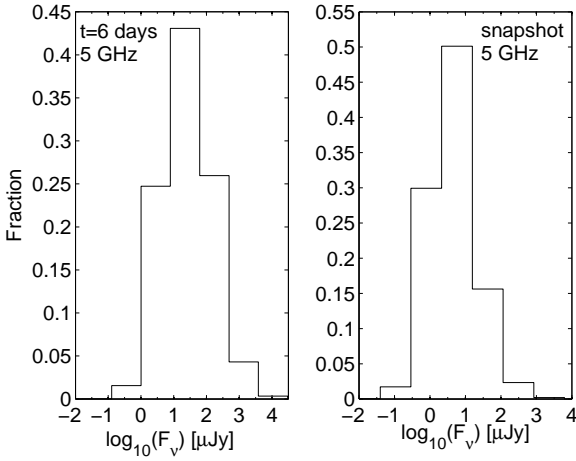


Figure 3. As Fig. 1 but for flux distributions in the radio band at 5 GHz frequency. Our left panel may be compared with fig. 6 of Berger et al. (2005)

observation epoch at a rate $R_{\text{obs}} \simeq 2195 \text{ yr}^{-1}$ for 10 years.² For each OA in a snapshot, we thus know the observed age, t_a .

We generate its redshift, z , according to the probability distribution discussed in § 2.1 and its viewing angle θ according to

$$P(<\theta) = (1 - \cos \theta), \quad (4)$$

with $0^\circ \leq \theta \leq 90^\circ$. From the matrix of the afterglow luminosities interpolated at $t_a/(1+z)$, θ and $\nu(1+z)$, we calculate the OA flux and compare it with a given flux threshold, F_{th} . We can, thus, compute the expected number of afterglows above F_{th} in a given band ν : $N_{\text{snap}}(> F_{\text{th}}, \nu)$. This is

² This expected rate of GRBs observed from the Earth is given by integrating $R_{\text{GRB}}/(1+z) = kR_{\text{SN}}/(1+z)$ over the whole volume of the universe.

the number that would be seen in a snapshot observation of the entire sky.

Model predictions for a flux limited survey require the calculations of two other quantities: the mean time spent by a OA above the flux limit,

$$\langle \log_{10} t_a \rangle = \frac{\sum_0^\infty \log_{10} t_a}{N_{\text{snap}}} \equiv \log_{10} T_{\text{th}}, \quad (5)$$

and the mean rate at which OAs appear in the sky over the survey flux threshold,

$$R_{\text{oa}} = N_{\text{snap}} \left(\frac{\sum_0^\infty t_a^{-1}}{N_{\text{snap}}} \right) \equiv \frac{N_{\text{snap}}}{T_{\text{rate}}}. \quad (6)$$

The resulting plots for N_{snap} , T_{rate} and T_{th} are shown in Figs 5, 6 and 7 (thick lines). They can be used to estimate the number of OAs expected in a given survey. If the observing time of a survey T_{obs} is shorter than the time T_{th} for which an afterglow is detectable, then we can consider it a snapshot observation and the total expected number of detected OAs is

$$N_{\text{oa}}(> F_{\text{th}}, \nu) = N_{\text{snap}}(> F_{\text{th}}, \nu) \frac{\Omega_{\text{obs}}}{4\pi}, \quad (7)$$

where Ω_{obs} is the solid-angle of the sky covered by the snapshot. Viceversa, the total expected number of OAs is computed as

$$N_{\text{oa}}(> F_{\text{th}}, \nu) = R_{\text{oa}}(F_{\text{th}}, \nu) T_{\text{obs}} \frac{\Omega_{\text{obs}}}{4\pi}. \quad (8)$$

Our results show that, as expected, the probability of detection and the mean duration above threshold increases with the survey sensitivity: to have a chance of detection in an all sky snapshot ($N_{\text{snap}} \gtrsim 10$) requires a flux limit of $\nu F_\nu \lesssim 10^{-14} [\text{erg cm}^{-2} \text{ s}^{-1}]$ at 1 keV, $R \gtrsim 23$ and $F_\nu \lesssim 1 \text{ mJy}$, at 5 GHz.

3 RESULTS

In the following, we first discuss how the main features of the USJ model affect the results, in comparison with the top-hat jet (§ 3.1). Then, we give specific predictions for a number of current and future surveys (§ 3.2).

3.1 “Orphan” afterglows in the USJ model and comparison with the “top-hat” model

TP02 performed detailed predictions for OAs in the TH case. They assumed that the whole GRB population is represented by 10 well-studied events. They used the observed opening angles (θ_{jet}) from afterglow breaks to constrain the comoving birth rate for each type. We may write the average comoving rate as $R_{\text{iso}}(z) \times \frac{4}{\langle \theta_{\text{jet}} \rangle^2}$, where R_{iso} is inferred from the prompt-emission, assuming that the co-moving rate is proportional to the star-formation rate. $R_{\text{iso}}(z)$ is equivalent to our $R_{\text{GRB}}(z)$. For the afterglow luminosity, TP02 used the observed (on-axis) afterglow lightcurves to compute the corresponding off-axis emission. Their results for a snapshot observation (thin lines) are compared to our predictions (thick lines) in Figs 5, 6 and 7. In all bands, their expected number of OAs (N_{exp} , solid thin line) is between one and two orders of magnitude larger than our N_{snap} (solid thick

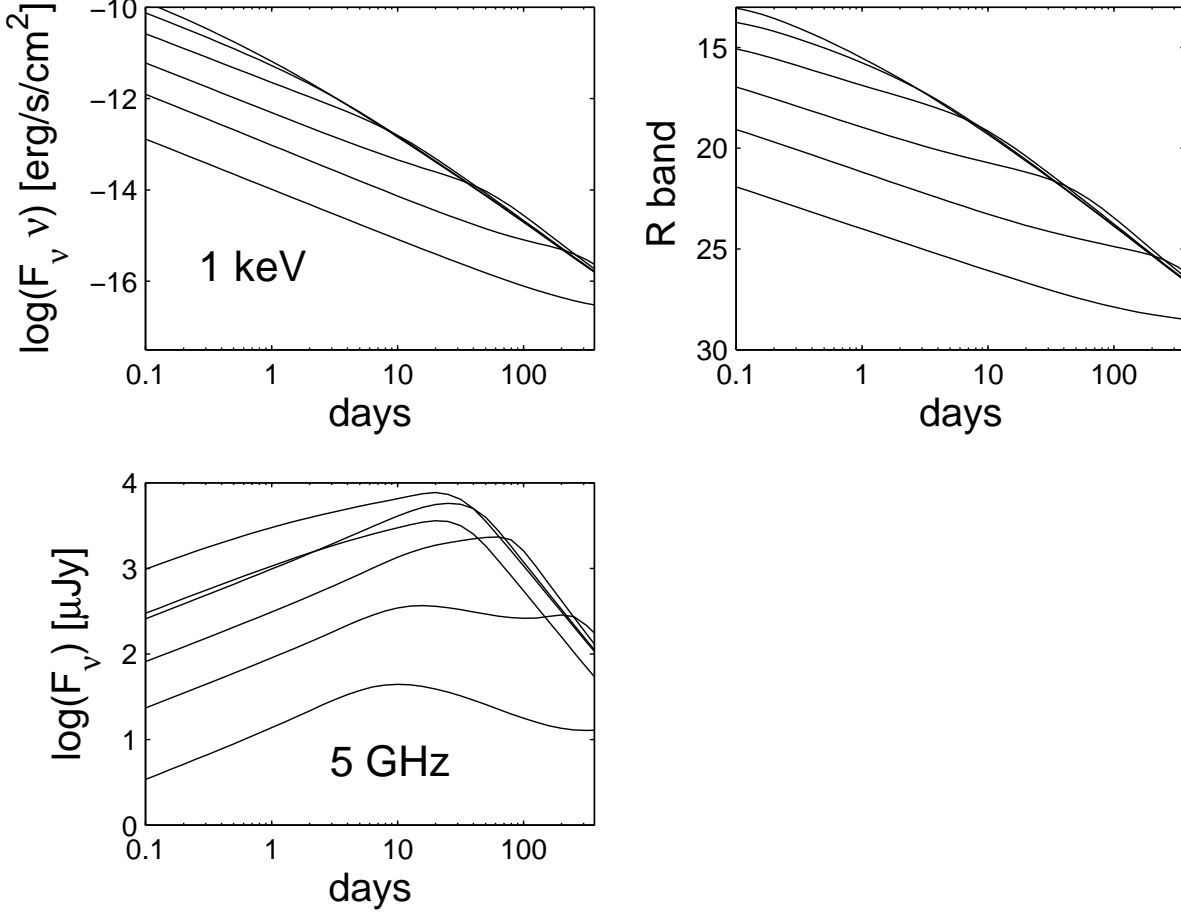


Figure 4. Afterglow lightcurves for a GRB at $z=1$ in X-ray (upper left panel), optical (upper right panel) and radio (lower left panel) bands. For each band, the different curves correspond to different viewing angles. From top to bottom, $\theta = 0^\circ, 4^\circ, 8.7^\circ, 19^\circ, 41.2^\circ, 90^\circ$.

line). They also made predictions for on-axis ($\theta \leq \theta_{\text{jet}}$) OAs (N_{on} , dotted thin line): at lower flux limits N_{on} becomes smaller than N_{snap} , while $N_{\text{on}} \gtrsim N_{\text{snap}}$ as the flux threshold increases.

This comparison highlights the two main differences between the models. The first is the presence of a geometrical beaming for the TH model. The mean angle of the 10 GRB prototypes is $\langle \theta_{\text{jet}} \rangle \sim 10^\circ$ (Panaitescu & Kumar 2002), thus the intrinsic comoving rate for their top-hat model is roughly $\frac{4}{\langle \theta_{\text{jet}} \rangle^2} \sim 130$ times higher than the USJ comoving rate. This also explains why $N_{\text{on}} < N_{\text{snap}} < N_{\text{exp}}$ as the sensitivity increases and detectability becomes less and less of an issue. In this limit, in fact, differences in the adopted afterglow flux distributions do not play an important role. Instead, the flux distribution does matter at high flux limits, where N_{on} becomes eventually greater than N_{snap} . This indicates that our flux distributions (Figs 1-3, right panels) have relatively more faint OAs than TP02 derived from the 10 afterglow prototypes. This may be due to the fact that those 10 afterglows are among the brightest. We, instead, chose our distribution to agree with a larger and probably less biased observed sample. Since in the two models the afterglow radiative efficiency (i.e. shock parameters and exter-

nal density) does not correlate with luminosity, the different relative number of bright OAs can be translated into underlying different luminosity functions. Ours is in fact steeper.

The average time above threshold (dubbed T for the TH jet) depends on the luminosity function and on the afterglow shape. On-axis OAs for the TH jet have qualitatively the same lightcurve shape as OAs in the USJ. The different luminosity function implies that their average persistence above threshold is longer or comparable to T_{th} for the same flux limit. Off-axis OAs, instead, have a different shape, since relativistic beaming suppresses the emission at early times, shortening their persistence above threshold. In this case $T \leq T_{\text{th}}$ for a given F_{th} . The comparison between the times (dashed lines) in Figs 5, 6 and 7 can then be understood. At low sensitivity, we select relatively more on-axis OAs ($N_{\text{exp}} \gtrsim N_{\text{on}} > N_{\text{snap}}$) and $T \geq T_{\text{th}}$. On the other hand, at high sensitivity the time average is dominated by off-axis afterglows ($N_{\text{exp}} \gg N_{\text{snap}} > N_{\text{on}}$) and $T \leq T_{\text{th}}$.

3.2 Specific surveys predictions

In this section, we provide illustrative predictions for various current and planned surveys. We use here the results shown

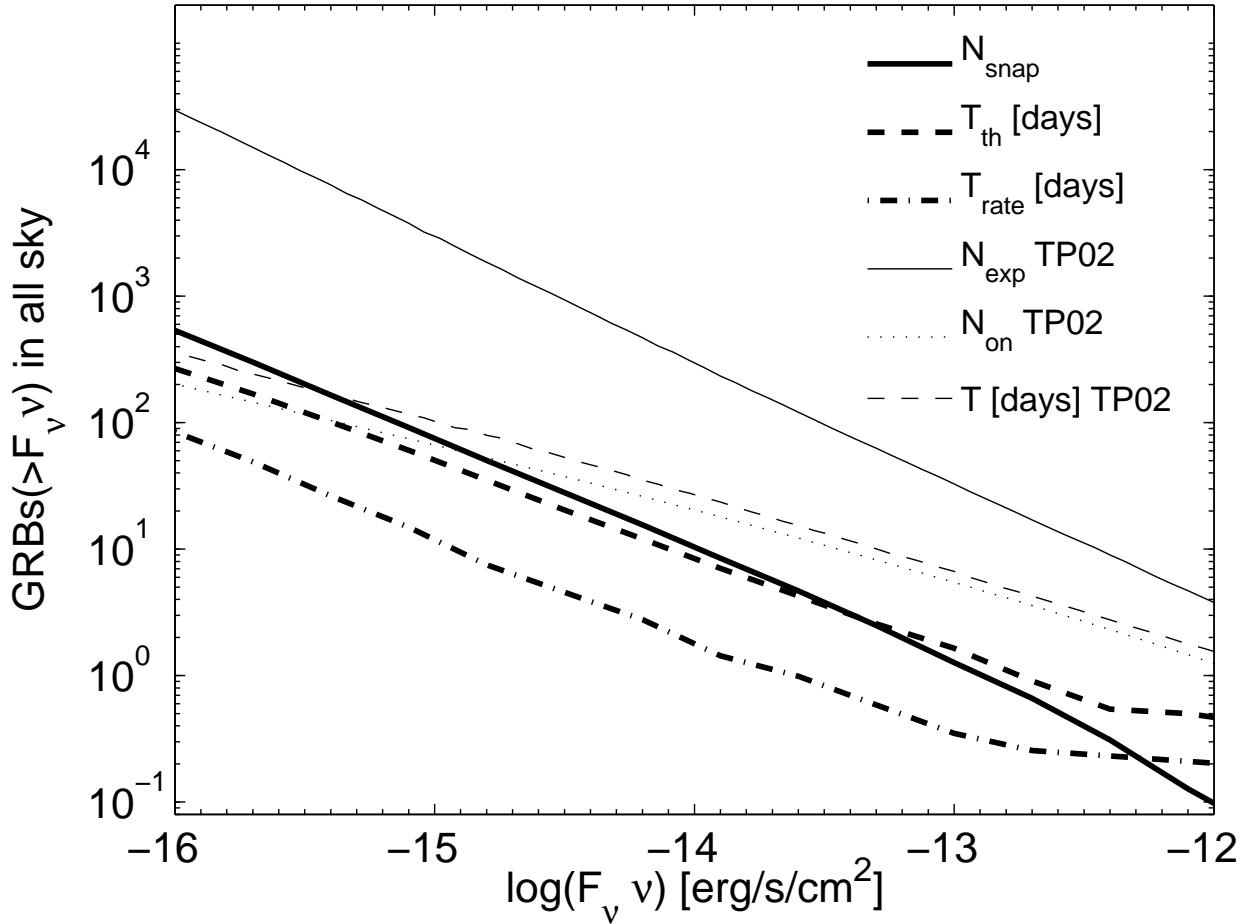


Figure 5. Expected number of afterglows in an all-sky snapshot observation in the X-ray band, as a function of the flux threshold. Both the predictions for the USJ model (thick solid line) and for the top-hat model (thin solid line, from PT02) are shown. For the USJ, we also plot T_{th} (thick dashed line) and T_{rate} (thick dot-dashed line) in days. For the TH model, we show from the same authors the expected afterglows detected on-axis (thin dotted line) and the mean time above threshold T in days (thin dashed line).

in Figs 5, 6 and 7. We note that those numbers should be taken as upper limits when compared with observations, since we did not consider detection limitations (e.g. host galaxy, dust absorption etc..) other than instrumental.

We also note that a detailed comparison between observation and theory requires knowledge of the specific survey strategies. However, generic conclusions can be drawn from the following examples.

3.3 X-ray

The two most sensitive X-ray surveys ($\sim 1 \times 10^{-15}$ [erg s $^{-1}$ cm $^{-2}$] in the 0.5-2 keV band) performed by *Chandra* and *XMM-Newton* are the 2 Msec Chandra Deep Field-North and the 0.8 Msec XMM-Newton Lockman Hole field. They cover respectively an area of 0.13 and 0.43 deg 2 . Since $T_{\text{th}} \simeq 52$ days, these surveys are equivalent to two snapshot observations. The small coverage of the sky results in a very small detection probability of a few 10^{-4} . Larger surveys, as the XMM-Newton Bright Serendipitous Source Sample

(Della Ceca et al. 2004) or The Chandra Multi-wavelength Project (ChaMP; e.g. Kim et al. 2007), are less sensitive ($\nu F_{\text{th}} \gtrsim 10^{-14}$ [erg s $^{-1}$ cm $^{-2}$]) and the increase in area is not sufficient to yield more than $N_{\text{oa}} \lesssim 10^{-2}$.

The ROSAT All Sky Survey (RASS; e.g. Voges et al. 1999) covers the full sky. The RASS exposure is 76435 deg 2 days, with a sensitivity of 10^{-12} [erg s $^{-1}$ cm $^{-2}$]. Therefore the survey is equivalent to an all sky observation with $T_{\text{obs}} = 1.85$ days. At this flux threshold, OAs are fast X-ray transients, lasting for $T_{\text{th}} \simeq 0.5$ days and $R_{\text{oa}} \simeq 0.5$ [day $^{-1}$]. Therefore, despite the large coverage of the sky, we predict that the survey should have found only $N_{\text{oa}} \simeq 0.9$. In fact, Greiner et al. (2002) found 23 OA candidates. After spectroscopic follow-up, however, they concluded that most, if not all events, are stellar flares. This is in agreement with our predictions.

The prospects for detection are not exciting even for the future mission eROSITA (extended ROentgen Survey with an Imaging Telescope Array). It will perform the first imaging all-sky survey up to 10 keV with a sensitivity of

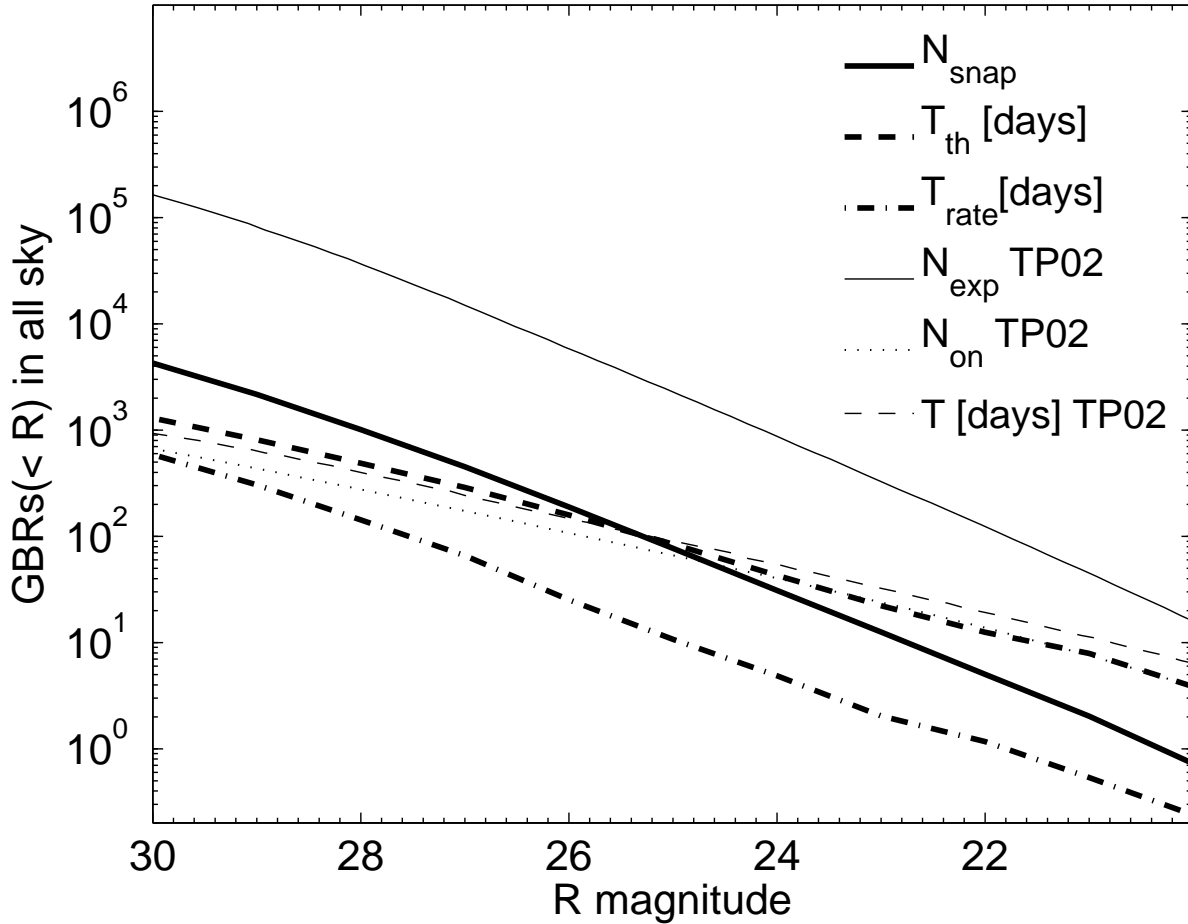


Figure 6. The same as Fig. 5, but for the R band.

5.7×10^{-14} [ergs $^{-1}$ cm $^{-2}$] in the 0.5-2 keV band. We predict 2.3 OAs.

These dispiriting results can be understood from Fig. 1 and Fig. 5: the flux limit should be $\lesssim 10^{-14}$ [erg s $^{-1}$ cm $^{-2}$] in order to have a good chance of detection in one all sky snapshot. To achieve such a sensitivity, a long exposure time is needed (e.g. ~ 50 ksec for Chandra). Given the small field of view of the current instruments, a full sky scan is unfeasible. We conclude that X-ray surveys are a poor tool for OA searches if jets are described by the USJ model.

The TP02 top-hat model predicts $N_{\text{exp}}/N_{\text{shot}} \sim 10 - 10^2$. This is not enough to yield detections in the *Chandra* and *XMM* current surveys. However, up to ~ 8 OAs should be present in the RASS. This might put some constraints on their model, if none of the Greiner et al. (2002) candidates are confirmed. More promising is the eROSITA mission that can yield up to ~ 56 OAs. The difference from the N_{oa} predicted by the USJ may be enough to put constraints on the models.

3.4 Optical

The most recent optical OA searches are the ones by Rau et al. (2006) and by Malacrino et al. (2007). Rau et al. observed 12 deg 2 of sky for 25 nights, separated by one or two nights. They used the MPI/ESO Telescope at La Silla, reaching $R=23$. Since at that sensitivity $T_{\text{th}} \simeq 22$ days and $T_{\text{rate}} \simeq 2$ days, we compute the expected OAs through an average rate of $R_{\text{oa}} = 6.3$ day $^{-1}$. We find $N_{\text{oa}} = 0.02$, considering an actual observing time of 12.5 days. Malacrino et al. used images from the CFHTLS very wide survey. They searched 490 deg 2 down to $R=22.5$. They observed 25-30 deg 2 every month over a period of 2-3 nights (Malacrino et al. 2006). Since $T_{\text{th}} \simeq 17$ days, we can consider their survey a snapshot observation and we predict $N_{\text{oa}} = 0.1$. Recently, Malacrino et al. (2007b) have rejected the only candidate they had identified in their first work and our predictions are now consistent with their result. The TH prediction of $N_{\text{exp}} = 2.4$ is still marginally consistent.

The most recent Sloan Digital Sky Survey (SDSS) data release (Adelman-McCarthy et al. 2007) includes imaging of 9583 deg 2 , with a R magnitude limit of 22.2. We expect $N_{\text{oa}} \simeq 1.5$. If we take a more conservative magnitude limit

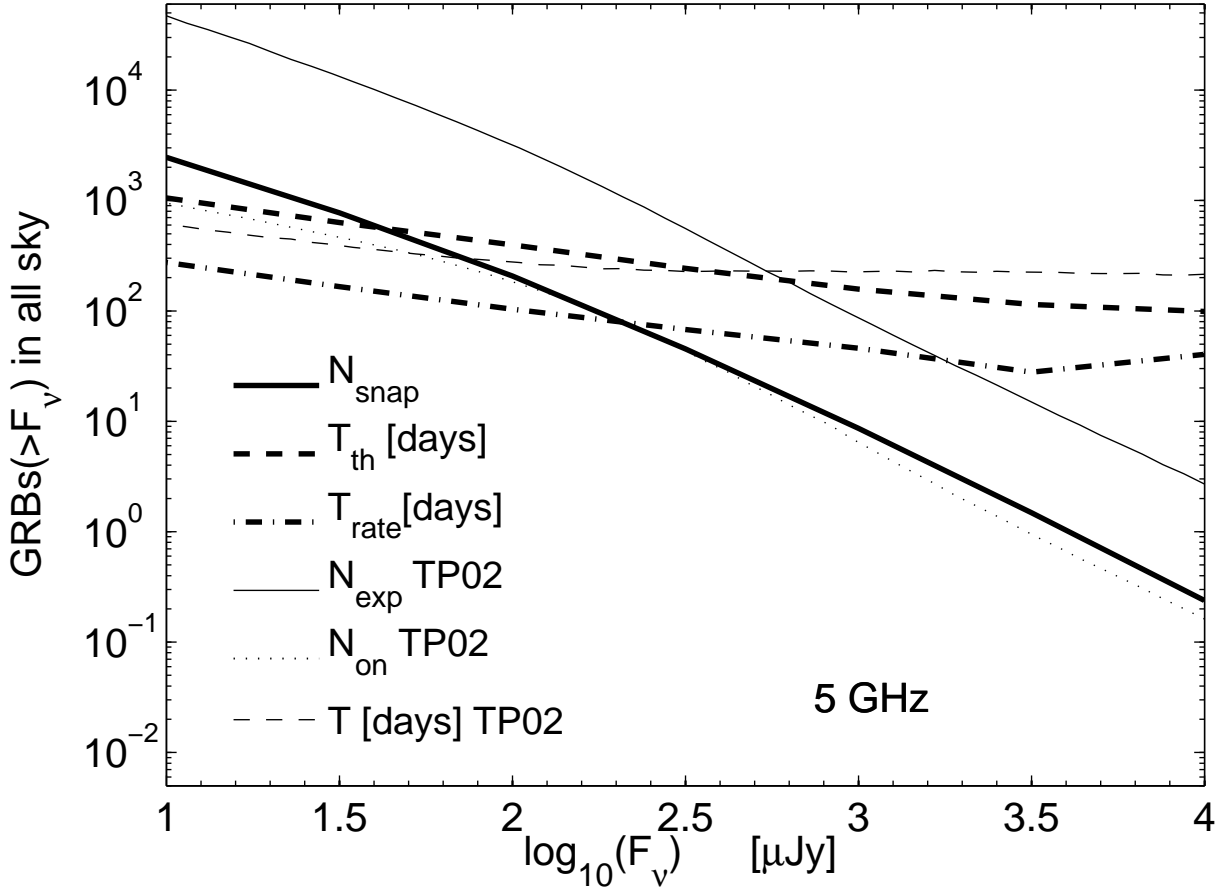


Figure 7. The same as Fig. 5, but for the radio band.

of 19 to account for the need for spectroscopic identification, the detection probability drops to ~ 0.05 .

The previous meagre results are due to the fact that a very large detection area is essential for these sensitivities (Fig. 2 right panel and Fig. 6). Only with the flux limit of the Subaru Prime Focus Camera ($R \simeq 26$ in 10 minutes of exposure), we could restrict ourselves to 5 % of the sky and get a snapshot with $N_{\text{oa}} \simeq 10$. This, however, would require a total observing time of $T_{\text{obs}} \simeq 57$ days.

Future larger surveys include GAIA (Parryman et al. 2000) and the Panoramic Survey Telescope & Rapid Response System (Pan-STARRS; e.g. Kaiser et al. 2002). The first is an all sky survey with a magnitude limit of $R \sim 20$. It will observe each part of the sky 60 times separated by one month (Lattanzi et al. 2000). At this sensitivity, an OA stays in the sky on average for 3.8 days; thus GAIA will perform 60 independent snapshots of the sky, with a prediction of $N_{\text{oa}} \simeq 44$. Pan-STARRS is expected to scan three-quarters of the entire sky in about a week, down to an apparent magnitude of 24. Since $T_{\text{th}} \simeq 43$ days, this can be considered a snapshot observation and we expect $\simeq 23$ OAs.

Thus, future optical surveys could be powerful tools for OA searches. Moreover, they could help to discriminate between the top-hat and the USJ models. In fact, the top-hat

model predicts that GAIA and Pan-STARRS would give respectively 953 and 657 OAs, an order of magnitude more OAs than predicted by the USJ!

3.5 Radio

Levinson et al. (2002) searched for transients by comparing the FIRST and NVSS (NRAO VLA Sky Survey) radio catalogues and found 9 candidates. Gal-Yam et al. (2005) rejected all candidates by means of follow-up radio and optical observations and placed an upper limit (95 % confidence) of 65 radio transients for the entire sky above 6 mJy at 1.5 GHz. This may be translated to a sensitivity threshold of 3.3 mJy at 5 GHz, using a typical late time spectral shape in radio of $F \propto \nu^{-0.5}$ (TP02). We predict $\simeq 1.4$ radio afterglows.

Recently, Bower et al. (2007) published an archival survey with data from the Very Large Array, spanning 22 years. For an effective area of 10 deg^2 , we get a rate of $\simeq 4 \times 10^{-2} \text{ yr}^{-1}$ for OAs brighter than $370 \mu\text{Jy}$. This rate is too low to account for the 10 detected transients. In addition the observed transient duration of approximately a week suggests that those sources are not indeed afterglows, which are ex-

pected to last above that threshold for approximately half a year.

Fig. 3 and Fig. 7 and the above examples show that the OA search would greatly benefit from lowering the survey sensitivity below 1 mJy, with an area of $\gtrsim 10,000 \text{ deg}^2$.

FIRST (Faint Images of the Radio Sky at Twenty-cm; Becker, White & Helfand 1995) will cover over 10^4 deg^2 of the North Galactic Cap. The survey area has been chosen to coincide with that of the SDSS. The sensitivity is $F_{\text{th}} \sim 1 \text{ mJy}$ at 1.4 GHz. This may be translated into a flux limit of 0.5 mJy at 5 GHz. If we consider, as for the SDSS, an area of 9583 deg^2 , we expect $\simeq 7$ OAs.

The Allen Telescope Array (ATA)³ is planned to observe 10^4 deg^2 at mJy sensitivity and later to go as deep as $\sim 0.1 \text{ mJy}$ at 5GHz. The expected number of OAs would then rise from a few to 50.

The top-hat model would predict 61 OAs for the FIRST survey and 735 OAs for the submillijansky ATA survey. This is again a favourable situation where a comparison with data may allow us to constrain the jet models.

4 DISCUSSION AND CONCLUSIONS

The realization that GRBs may be jetted has triggered studies of orphan afterglows. Early studies assumed that the prompt GRB emission comes from a sharp jet, in which case the ratio of afterglows to that of GRBs yields a constraint on the GRB beaming fraction (or equivalently the opening angle of the GRB jet). This parameter is of importance for a proper assessment of GRB rates and energetics.

The structured jet model has offered an equivalent explanation for afterglow phenomenology. However, its interpretation of the lightcurve breaks is different: they would arise from viewing angle effects and not from geometrical collimation. In fact, if GRB jets are indeed structured, most, if not all, afterglows should be generally preceded by a prompt emission pointing towards the observer. Therefore, even if in practice the relative number of detections in various bands depends on the survey strategy, the ratio should tend to unity ($b = 1$) if events are detectable at arbitrarily low fluxes.

The different geometrical configuration also means that, for the same observed GRB rate, the intrinsic birth rate is ~ 100 times higher for the top-hat model. At low detection threshold, where instrumental selection effects are minimized, this higher rate results in an excess of predicted OAs with respect to the USJ. On the other hand, for high detection thresholds, the relative number of OAs in the two models is mainly due to the afterglow flux distribution.

With respect to detection prospects in the USJ framework, we conclude that large sky coverage is essential in all bands. In addition, X-ray and radio instruments should push their flux limit below $10^{-14} [\text{erg s}^{-1} \text{ cm}^{-2}]$ (at 1 keV) and $\sim 1 \text{ mJy}$ (at 5 GHz) respectively. Current and planned X-ray surveys are thus not suited for OAs searches, if the jet is structured. However, the future X-ray mission eROSITA could discriminate between the jet models, since if the jet is

TH, it could detect tenths of OAs. The FIRST and the future ATA projects could be successful in detecting radio OAs and constrain jet models, since $N_{\text{exp}}/N_{\text{snap}} \simeq 10$. The potential is even better for future optical all-sky surveys, such as GAIA and Pan-Starrs, since the difference in the expected event numbers is higher, $N_{\text{exp}}/N_{\text{snap}} \sim$ a few tens. We also note that it would be worthwhile to exploit the great sensitivity of the Suprime-Cam, for which 5-10% of the whole sky is sufficient for positive detections. Certainly, a combination of X-ray, optical and radio observations would yield the most of information.

ACKNOWLEDGMENTS

We are very grateful to T. Totani and A. Panaitescu for providing us with their data for the TH predictions. We also acknowledge very useful discussions with G. Bower and E. Nakar. EMR acknowledges support from NASA through Chandra Postdoctoral Fellowship grant number PF5-60040 awarded by the Chandra X-ray Center, which is operated by the Smithsonian Astrophysical Observatory for NASA under contract NASA8-03060.

REFERENCES

- Adelman-McCarthy, et al., 2007, arXiv0707.3413A
- Barrow, D. N, Racusin, J., 2006, arXiv:astro-ph/0702633
- Becker, A. C., Wittman, D. M., Boeshaar, P. C., et al. 2004, ApJ, 611, 418
- Becker, R.H., White, R.L., & Helfand, D.J., 1995, ApJ450, 559
- Berger, E. et al., 2005, ApJ, 634, 501
- Daigne, F., Rossi, E. M., Mochkovitch, R., 2006, MNRAS, 372, 1034
- Della Ceca, R., et al. 2004, A&A, 428, 383
- Greiner, J., Hartmann, D. H., Voges, W., Boller, T., Schwarz, R., Zharikov, S. V., 2000, A&A, 353, 998
- Frail D. A., et al., 2001, ApJ, 562, 55
- Gal-Yam et al, 2006, ApJ, 639, 331
- Greiner, J., Hartmann, D. H., Voges, W., Boller, T., Schwarz, R., Zharykov, S. V., 2002, AIPC, 526, 380
- Grindlay, J. E., 1999, ApJ, 510, 710
- Hopkins, A. M., 2004, ApJ, 615, 209
- Kaiser, N., et al., 2002, SPIE, 4836, 154
- Kim, M., et al., 2007, ApJS, 169, 401
- Kommers, J. M., Lewin, W. H. G., Kouveliotou, C., van Paradijs, J., Pendleton, G. N., Meegan, C. A., Fishman, G. J., 2000, ApJ, 533, 696
- Lattanzi, M. G., Spagna, A., Sozzetti, A., Casertano, S., 2000, MNRAS, 315, 211L
- Levinson, A., Ofek, E. O., Waxman, E., Gal-Yam, A., 2002, ApJL, 576, 923
- Malacrino, F., Atteia, J. L., Boer, M., Klotz, A., Veillet, C., & Cuillandre, J. C., 2007, A&A, 464L, 29
- Malacrino, F., Veillet, C., Atteia, J. L., Boer, M., Cuillandre, J.-C., Klotz, A., Withington, K., 2007b, GCN, 6581, 1M
- Malacrino, F., Atteia, J. L., Boer, M., Klotz, A., Veillet, C., & Cuillandre, J. C., 2006, A&A, 459, 465
- Macfadyen, A. & Woosley, S. 1999, ApJ, 524, 262

³ See e.g. <http://ral.berkeley.edu/ata/science/>.

- Mészáros, P. & Rees, J. M. ,1997, ApJ, 476, 232
- Nakar, E., Piran, T., & Granot, J., 2002, ApJ, 579, 699
- Nakar, E. & Piran, T., 2003, New Astr., 8, 143
- Nousek, J. A., 2006, ApJ, 642, 389
- Panaitescu, A., Kumar P., 2000, ApJ, 543, 66
- Panaitescu, A., Kumar P., 2001, ApJ, 554, 667
- Panaitescu, A., Kumar P., 2002, ApJ, 571, 779
- Panaitescu, A., Kumar P., 2004, MNRAS, 350, 213
- Perna, R. & Loeb, A. 1998, ApJL, 509, 85
- Perryman, M. A. C., et al., 2001, A&A, 369, 339
- Porciani C., Madau P., 2001, ApJ, 548, 522
- Preece, R. D., Briggs, M. S., Mallozzi, R. S., Pendleton, G. N., Paciesas, W. S., Band, D. L., 2000, ApJS, 126, 19
- Rau, A., Greiner, J., Schwarz, R. 2006, A&A, 449, 79
- Rhoads, J. 1997, ApJL, 487, 1
- Rossi, E. M., Lazzati, D. & Rees, M. J. 2002, MNRAS, 332, 945
- Rossi, E. M., Lazzati, D., Salmonson, J. D., Ghisellini, G., 2004, MNRAS, 354, 86
- Rykoff, E. S., Aharonian, F., Akerlof, C. W., et al. 2005, ApJ, 631, 1032
- Sakamoto, T., et al., 2005, ApJ, 629, 311
- Sari, R. & Piran, T., 1999, ApJ, 520, 641
- Schaefer, B. E. 2002, in “Gamma-Ray Burst and Afterglow Astronomy” 2001, Ed. G. Ricker et al. (Woodbury, AIP)
- Spergel, D. N., 2007, ApJS, 170, 377
- Stern, B. E., Atteia, J.-L., Hurley, K., 2002, ApJ, 578, 304
- Stern, B. E., Tikhomirova, Y., Stepanov, M., Kompaneets, D., Berezhnoy, A., Svensson, R., 2000, ApJL, 540, L21
- Totani, T. & Panaitescu, A. 2002, ApJ, 576, 120
- Vanden Berk, D. E. et al., 2002, ApJ, 576, 673
- Voges, W et al., 1999, A&A, 349, 389
- Zhang, B. & Meszaros, P. 2002, ApJ, 571, 876
- Zou, Y. C., Wu, X. F., & Dai, Z. G., 2007, A&A, 461, 115